

On the Role of Dissipation in Inertial Western Boundary Currents

PETER D. KILLWORTH

Institute of Oceanographic Sciences, Deacon Laboratory, Wormley, Godalming, Surrey, England

(Manuscript received 25 October 1991, in final form 8 May 1992)

ABSTRACT

The problem of matching the nonlinear, frictional flow in a simple western boundary layer to a specified interior flow is considered. Two problems are discussed, using streamfunction as a coordinate across the boundary layer. First, a unidirectional flow is considered. The dissipation is considered to be some positive quantity, and it is shown that for a simple form of this, many different amounts permit a smooth match to the interior. The magnitude of the dissipation can be determined absolutely at the dividing point between in- and outflow. The dissipation south of this point must be smaller and north of this point must be larger; a simple equation describes the relationship between dissipations north and south of the dividing point. Second, a bidirectional boundary layer is permitted. A specific form of dissipation (a linear drag) is applied, with a constant coefficient. It is shown that in this case it still remains possible to match to a specified interior flow, although inertial overshoot occurs both into the next gyre polewards as well as equatorwards into the inflow region, if the drag is small enough. Thus, taken together with published results on Laplacian dissipation, these simple models suggest that western boundary layers are passive and can match to a specified interior flow without modifying that flow in any way (although this may not be the case for very low friction).

1. Introduction

The precise role played by a western boundary layer in the gyre in which it is embedded is far from clear. Early studies by Stommel (1948) and Munk (1950) demonstrated that a narrow dissipative western region was necessary to remove the continuous input of vorticity by the wind over the gyre (for example, cf. Pedlosky 1987). However, when the dissipative term takes only a small value, the western boundary layer must take a convoluted form in order that the dissipation can occur over a sufficient length of streamline to achieve the correct energy balance. This leads inevitably to the requirement for a strong recirculation region (e.g., Cessi et al. 1990). If the dissipative term is somewhat larger there is no need for a recirculation region, and a simple unidirectional western boundary current can occur.

The formal difficulty with such a boundary current is that the predominant momentum balance is inertial, that is, nonlinear. Steady, nonlinear, dissipationless boundary-layer theories were developed by Charney (1955) and Morgan (1956). These theories are capable of giving a good description of the southern half of an anticyclonic gyre—that is, the part that involves an inflow from the interior of the gyre to the western boundary current. Because of the necessity to balance

vorticity input with dissipation, these theories fail in the northern half of the gyre where the flow leaves the western boundary current in an eastward direction and rejoins the interior. The failure manifests itself most clearly in the inability of the solutions to maintain two conserved quantities simultaneously on the same streamline: a Bernoulli functional and potential vorticity. In the simplest case, the Bernoulli functional is just the upstream pressure head and is related to a layer depth, while the potential vorticity is related to both the Coriolis parameter and the layer depth. Clearly both cannot be conserved simultaneously if a latitude change is involved except in unusual circumstances (e.g., uniform potential vorticity solutions pioneered by Fofonoff 1954).

These difficulties have meant that most studies of western boundary layers have been numerical in some form. Such studies have usually, by necessity, included the solution of the essentially dissipation-free interior as well as the western boundary layer.

Dissipation is caused by a variety of effects: time-dependent barotropic–baroclinic eddy and interactions with the ocean floor and walls. Only recently have basin-scale eddy-resolving numerical models been able to resolve the eddy structure of a western boundary current (Bryan and Holland 1989), so that most studies have continued to parameterize the effect of eddies in some way. These parameterizations are ad hoc, partly because the numerical models fail without such terms; they include linear drag (Stommel) terms, Laplacian drag (Munk), and biharmonic and higher terms. The

Corresponding author address: Dr. Peter D. Killworth, Robert Hooke Institute, The Observatory, Clarendon Laboratory, Parks Road, Oxford, OX 1 3PU England.

boundary conditions required for such terms (no-slip, free-slip, superslip, etc.) become equally ad hoc and the subject of debate. Many parameterizations imply a downgradient transfer of the property being mixed—usually momentum, but more properly potential vorticity—yet there is little direct evidence for the direction or size of mixing in, say, the Gulf Stream. The behavior of different physical systems, for example, the strong boundary current separation of quasigeostrophic models versus the tendency for primitive equation models to separate rather less, is also under investigation.

For the near future, then, we must continue to study western boundary layers using simple frictional forms. We do so not because we have confidence in them, but because we have nothing better to date (and, also, because their effects are somewhat simpler to understand).

There is another linked problem. Studies of the interior geostrophic thermohaline circulation (cf. Weiland 1971 for a survey) were wind and buoyancy driven and explicitly ignored the role of the western boundary layer. This neglect has continued, both with layered models (Luyten et al. 1983) and continuously stratified models (Killworth 1987; Huang 1986). In all cases the western boundary layer was presumed entirely passive and capable of accepting and returning any fluid sent into it from the interior.

This assumption is both necessary and worrying for such models: necessary because geostrophy precludes the dynamics appropriate to the boundary layer and worrying because there is as yet little proof that the boundary layer is capable of behaving in the manner required by the theories. Specifically, how easily can the western boundary layer match onto an arbitrary geostrophic interior?

The question partly depends on the form of dissipation employed. Cessi et al. (1990) use a small Laplacian dissipation in a highly idealized study and find, as in Moore's (1963) model, that their solution can eventually match to a specified interior flow, together with standing planetary waves. In this case the along-boundary component of the boundary-layer flow is alternately positive and negative as one moves eastward towards the interior. The "interior" here is only (part of) the region of outflow from the western boundary layer; the inflow portion of the interior is assumed to have created a specified boundary layer. Has the fourth-order nature of Cessi et al.'s equation set given enough degrees of freedom so that the match with the interior is successful? What if the dissipation term took another form, for example, a simple linear drag? If the coefficient of this drag is sufficiently large, then the planetary wave regime disappears and the alongboundary flow is of one sign everywhere. Can solutions in this case match onto an arbitrary interior?

We examine two linked questions in this paper, using a simple model. We let the dissipation be a positive definite quantity, defined as the first term in a Taylor

series from a value of zero in the fluid interior (but otherwise not linked to flow variables in any way). We examine various forms for the coefficient of this quantity and show that values in the outflow region are specified, while values in the inflow region can be freely chosen. Accordingly, many different *amounts* of dissipation permit a western boundary current to match with a specified interior flow structure. This is rather surprising: even within the simple dynamics, the solutions permits a nonunique western boundary current.

However, this could be a product of the free form permitted for the dissipation. This will be shown not to be the case. We then (section 5) specify that the dissipation takes the form of a linear drag with a constant coefficient. It turns out that the western boundary current can still be matched to a specified interior, for any dissipation, although when the dissipation becomes small, two new features occur: the boundary-layer flow becomes bidirectional and inertial overshoot occurs both into the next gyre polewards and into the westward-flowing interior to the south. This latter effect causes unresolved difficulties in defining what is meant by the "interior" circulation.

2. The problem

For simplicity we choose a steady $1\frac{1}{2}$ -layer model, driven by an Ekman pumping w_E . Taking axes x eastward and y northward, the momentum and mass equations are, respectively,

$$uu_x + vv_y - fv = -g'h_x \quad (1)$$

$$uw_x + vv_y + fu = -g'h_y - D \quad (2)$$

$$(hu)_x + (hv)_y = -w_E, \quad (3)$$

where the velocity field is (u, v) , g' is a reduced gravity, and the depth of the fluid is denoted by h . The Coriolis term is $f(y) = f_0 + \beta y$. The dissipation is denoted by D . Suffixes denote partial differentiation, although later a prime will be used when the quantity concerned is only a function of a single variable.

The scaling for the problem is traditional. The interior fluid (i.e., that away from the western boundary layer) is assumed in geostrophic balance. Thus, if L is a typical length scale, we find that in the interior

$$h \sim H = f_0 \left(\frac{Lw_E}{\beta g'} \right)^{1/2}, \quad u, v \sim U = \frac{g'H}{f_0 L}. \quad (4)$$

In the western boundary layer the balance is semi-geostrophic. Here the northward velocity is of order $(g'H)^{1/2} \gg U$, whereas the eastward velocity is of order U as before. The thickness of the boundary layer is the deformation radius $a = (g'H)^{1/2}/f_0$. [This can also be written as $(ULf_0^{-1})^{1/2} \sim (U\beta^{-1})^{1/2}$, which is the more familiar form due to Charney (1955).] To leading order, then, the momentum and mass equations become

$$-fv = -g'h_x \tag{5}$$

$$uv_x + vv_y + fu = -g'h_y - D \tag{6}$$

$$(hu)_x + (hv)_y = 0, \tag{7}$$

where the omitted terms are all small, as can easily be verified. Notice that the dissipation has been retained only in (6); in (5), it is of order $(a/L) \ll 1$ compared with the geostrophic terms. Also, the form of the dissipation has not been specified. These equations can now be nondimensionalized using the above scalings. Explicitly, put $u = Uu'$, $v = (g'H)^{1/2}v'$, $h = Hh'$, $y = Ly'$, $x = ax'$, $D = (g'H/L)D'$, and then drop the primes. This yields

$$-(1 + \epsilon y)v = -h_x \tag{8}$$

$$uv_x + vv_y + (1 + \epsilon y)u = -h_y - D \tag{9}$$

$$(hu)_x + (hv)_y = 0, \tag{10}$$

where

$$\epsilon = \frac{\beta L}{f_0} \tag{11}$$

is the small—but not very small—variation in Coriolis parameter and

$$f = 1 + \epsilon y \tag{12}$$

is the Coriolis parameter itself. As typical values, we take $w_E \sim 10^{-6} \text{ m s}^{-1}$, $g' \sim 0.01 \text{ m s}^{-1}$, $f_0 \sim 10^{-4} \text{ s}^{-1}$, $\beta \sim 10^{-11} \text{ m}^{-1} \text{ s}^{-1}$, and $L \sim 2000 \text{ km}$. This yields $H \sim 450 \text{ m}$, $U \sim 0.02 \text{ m s}^{-1}$, and $\epsilon \sim 0.2$. The scaling for the northward boundary-layer velocity v is then 2 m s^{-1} and for the dissipation D is 10^{-6} m s^{-2} . (If the dissipation took the form κv , a scaling for κ would be 10^{-6} s^{-1} .)

From these equations we can deduce that the potential vorticity

$$q = \frac{f + v_x}{h} \tag{13}$$

is conserved apart from dissipative effects:

$$uq_x + vq_y = -\frac{D_x}{h}. \tag{14}$$

We may define a streamfunction ψ from (10) by

$$uh = -\psi_y, \quad vh = +\psi_x. \tag{15}$$

However, the set (8), (9), and (15) remains fully nonlinear and solutions are difficult to obtain. For this and the next two sections, we shall simplify the problem by making the assumption that the northward velocity v in the boundary layer is everywhere positive (so that ψ is monotonically increasing with x). In this case, we may use ψ as an independent variable in place of x (this Von-Mises technique has been used in many problems—e.g., Foster 1985; Huang 1990; Page and

Johnson 1991; Killworth 1992; the choice is convenient because ψ is a conserved quantity). The technique has the (apparent) disadvantage of precluding a recirculation region and, therefore, requires that the solution in the limit of large x , as the interior is approached, must possess a monotonic v velocity. This in turn constrains the form of the dissipation used (cf. the Appendix for details). However, a technique employed by Page and Johnson (1991) permits small dissipations and bidirectional v fields; this is postponed to section 5.

We thus use ψ and y as independent variables. Then (15) are transformed into

$$uh = \frac{x_y}{x_\psi} \tag{16}$$

$$vh = \frac{1}{x_\psi}, \tag{17}$$

while cross-stream geostrophy (8) yields

$$fv = \frac{h_\psi}{x_\psi}. \tag{18}$$

Equation (16) merely defines u when other quantities are known. Equations (17) and (18) may be combined to give

$$hh_\psi = f \tag{19}$$

or, integrating, we obtain an expression for h

$$h^2 = h_I^2(y) + 2f[\psi - \psi_I(y)]. \tag{20}$$

Here we have made implicit use of the boundary conditions for the problem. These are that $x = 0$ when $\psi = 0$ (at the western boundary), and that

$$x \rightarrow \infty, \quad v \rightarrow 0, \quad h \rightarrow h_I(y) \quad \text{as} \quad \psi \rightarrow \psi_I(y). \tag{21}$$

The quantities h_I and ψ_I are specified by the interior solution and are assumed known. They are connected by the geostrophic relations

$$fu_I(y) = -h_{Iy}, \tag{22}$$

$$\psi_{Iy} = -h_I u_I. \tag{23}$$

Here we shall assume that the region of interest is a single gyre, indicated schematically in Fig. 1 in both x and ψ coordinates. The gyre is assumed to have a southern boundary at $y = y_0$, where ψ vanishes. There is inflow from the interior up to $y = y_1$, at which point u_I vanishes. At this point ψ_I and h_I take their maximum values, ψ_m and h_m , say. Northward of y_1 , u_I is positive, representing outflow to the interior; ψ_I now decreases with y , reaching zero at the northward extent of the gyre, $y = y_n$.

There is an interesting deduction to be made from (20). Differentiation w.r.t. y , and use of (22), (23), gives

$$hh_y = \epsilon(\psi - \psi_I) < 0,$$

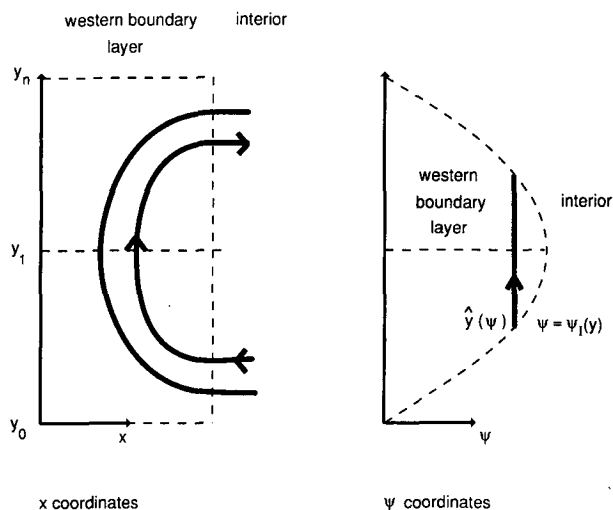


FIG. 1. The configuration used in the first part of this study. The left-hand diagram shows the situation in (x, y) space; the right-hand diagram shows the same situation, but in (ψ, y) space. The thick lines show streamlines in each coordinate system. The right-most dashed line indicates the boundary with the interior (in the x -coordinate case this boundary is formally at infinity).

so that h decreases northwards on *all* streamlines (despite the fact that h_{Iy} takes both signs). In other words, “water flows downhill.”

Conversion of the potential vorticity equation (14) gives

$$q_y = -D_\psi \tag{24}$$

after a little manipulation, so that q only changes along a streamline when D is both nonzero and varying with ψ . The final equation to be converted is the y -momentum equation (9), which becomes

$$vv_y + h_y + D = 0. \tag{25}$$

[Thus, if there were no-slip boundary conditions at $x = \psi = 0$ then (25), plus the fact that h_y is negative, shows that D would have to be positive definite on the western boundary. We shall not consider this case further.] Let us write

$$D = E_y \tag{26}$$

so that (25) is immediately integrable, to give conservation of energy

$$\frac{1}{2} v^2 + h = -E + B(\psi), \tag{27}$$

where $B(\psi)$ is the (as yet unknown) Bernoulli function. The definition of E needs a little care, since by (24) and (27) we can write

$$q + E_\psi = B'(\psi), \tag{28}$$

where a prime denotes differentiation w.r.t. the only dependent variable. Thus, in the absence of friction q

= $B'(\psi)$ as usual. In fact, it turns out that there is sufficient freedom to choose the integration constants in E so that it can be *defined* for our purposes as

$$E = \int_{y_0}^y D dy, \tag{29}$$

where

$$D \geq 0, \quad \psi \leq \psi_I(y)$$

$$D = 0, \quad \psi > \psi_I(y).$$

Equation (27) then serves as a definition of v , once the form of B is known, and together with (18), defining x_ψ , and (17), defining u , mean that for any given dissipation D , the problem is completely solved. Note that E , the integrated drag, appears as an effective topographic term in (27), so that too large a drag means that the fluid cannot pass over the “topography” E in a hydraulic sense.

We must now determine $B(\psi)$ and, hence, find out what restrictions must be placed on the form and size of D . Here, B will be set by the boundary conditions imposed at the boundary layer–interior junction where $\psi = \psi_I(y)$.

First, consider the southern half of the gyre $y \leq y_1$. We define the inverse of $\psi = \psi_I(y)$ to be $y = \hat{y}(\psi)$ as indicated in Fig. 1 (note that this functional refers to the *southern* of the two values of y with that value of ψ), for later convenience. At such a point, E is identically zero, since D vanishes in the interior. The northward velocity v also vanishes since this is the edge of the boundary layer. Then (27) reduces to

$$h_I(y) = B(\psi_I(y)), \tag{30}$$

which defines $B(\psi)$ completely, since $\psi_I(y)$, $y \leq y_1$ takes all permissible ψ values. From (30) we may differentiate w.r.t. y to find

$$B'(\psi_I) \cdot \psi'_I(y) = h'_I(y)$$

or

$$B'(\psi_I) = \frac{f}{h_I} = q_I(y), \quad y \leq y_1, \tag{31}$$

where the interior potential vorticity q_I has its linear value. So in a sense, the southern half of the gyre (the inflow) sets the boundary conditions, and the friction plays no role in this.

In the northern (outflow) part of the gyre, (27) gives at the junction with the interior

$$h_I(y) = -E(\psi_I(y), y) + B(\psi_I(y)). \tag{32}$$

From its definition,

$$\begin{aligned} E(\psi_I(y), y) &= \int_{y_0}^y D(\psi_I(y), y') dy' \\ &= \int_{\hat{y}(\psi_I(y))}^y D(\psi_I(y), y') dy', \end{aligned}$$

since D vanishes for the intermediate values of y . Substitution into (27), and differentiation w.r.t. y gives, using the fact that D vanishes at the boundary with the interior,

$$h'_I(y) = -\psi'_I(y) \int_{\hat{y}(\psi_I)}^y D_\psi(\psi_I(y), y') dy' + B'(\psi_I)\psi'_I(y), \quad (33)$$

where $\psi_I = \psi_I(y)$.

Equation (33) is an integral equation for the dissipation D . Its limits are interesting. They are, for any given ψ [i.e., any $\psi_I(y)$], precisely the two endpoints of the streamline within the boundary layer. Imagine that we have solved (33) for values of ψ near the maximum ψ_m , which involves only a small range of y values. Then as ψ decreases (i.e., moving westwards), values of D are introduced simultaneously at two new values of y . This suggests that values of D at one of these positions are somehow arbitrary: that it is only the combination of the two values that has a dynamic effect on the flow. We shall see below that this is indeed the case.

3. The solution for linear D

To proceed further, we need to specify the form of D . In this section we shall assume that D is given by a form general enough to permit solutions, but one that does not depend directly on other flow variables, for example, v . Now D vanishes as $\psi \rightarrow \psi_I$, so that a natural form is the first term in a Taylor expansion, namely,

$$D(\psi, y) = \alpha(y)(\psi_I(y) - \psi), \quad \psi \leq \psi_I(y), \quad (34)$$

and D vanishes otherwise. Here $\alpha(y)$ is a coefficient to be determined. For more general forms of friction, (34) remains the first term in the Taylor series, and so the discussion below would remain valid at least "near" the interior, providing the western boundary current was unidirectional. Substituting (34) into (33) yields

$$\int_{\hat{y}(\psi_I(y))}^y \alpha(y') dy' = \frac{h'_I}{\psi'_I} - B'(\psi_I) = \frac{f}{h_I} - B'(\psi_I), \quad y > y_1 \quad (35)$$

(note that when $y < y_1$ both sides are identically zero). Thus, if $\alpha(y)$ is specified for $y \leq y_1$, (35) defines $\alpha(y)$ for $y > y_1$ (or vice versa).

It is possible to calculate $\alpha(y_1)$ directly. Differentiating (35) w.r.t. y at $y \sim y_1$, we have

$$\alpha(y) - \hat{y}'(\psi_I)\psi'_I(y)\alpha(\hat{y}) = \left[\frac{d}{dy} \left(\frac{f}{h_I} - B'(\psi_I) \right) \right]_{y=y_1}. \quad (36)$$

Now $\hat{y}'(\psi_I(y)) = 1/\psi'_I(\hat{y})$ from the definition of \hat{y} . Also, as y nears y_1 the solution varies quadratically

about y_1 , and we have $\psi'_I(y) \sim -\psi'_I(\hat{y})$, so that (36) becomes

$$2\alpha(y_1) = \left[\frac{d}{dy} \left(\frac{f}{h_I} - B'(\psi_I) \right) \right]_{y=y_1}. \quad (37)$$

The first term on the rhs is merely ϵ/h_m . The second term, $-B''(\psi_m)\psi'_I(y_1)$, is apparently zero since ψ'_I is zero there. However, B'' has a square root singularity at ψ_m . [This is clear from differentiating (31) at $y = y_1$.] It is straightforward to show that

$$B''(\psi) \sim \frac{\epsilon}{h_m [2|\psi''_m|(\psi_m - \psi)]^{1/2}} \quad \text{as } \psi \rightarrow \psi_m,$$

which means that

$$\frac{d}{dy} (B'(\psi_I)) = -\frac{\epsilon}{h_m} \quad \text{as } \psi_I \rightarrow \psi_m.$$

Put together, this gives

$$\alpha(y_1) = \frac{\epsilon}{h_m} \quad (38)$$

after a little algebra.

This result shows that *whatever the form of the dissipation*, it must take the known value (38) at y_1 . This value increases with the beta effect (ϵ), which is to be expected since a stronger beta term means that the value of q on the outflow will have changed more markedly from its value on the inflow, necessitating more friction.

We now need to find α for other values of y . Either the integral equation (35) can be used, or else its differential. The latter case yields

$$\alpha(y) - \alpha(\hat{y}) \frac{\psi'_I(y)}{\psi'_I(\hat{y})} = \frac{d}{dy} \left(\frac{f}{h_I} - B'(\psi_I) \right), \quad y > y_1. \quad (39)$$

In this equation the ψ_I are all known, as are the h_I . Hence (39) provides a linear relation between $\alpha(y)$ and $\alpha(\hat{y})$.¹ One of these two may be chosen arbitrarily (although one would surely wish for continuity in α), but the other is then specified.

It is straightforward to see that under almost all conditions, the rhs of (39) increases with y , from a value of $2\alpha(y_1)$ when $y = y_1$. Further, $-1 < \psi'_I(y)/\psi'_I(\hat{y}) < 0$. Thus, (39) becomes

$$\alpha(y) + \sigma\alpha(\hat{y}) > 2\alpha(y_1), \quad y > y_1,$$

where $0 < \sigma < 1$. So, one or both of $\alpha(y)$, $\alpha(\hat{y})$ must be greater than $\alpha(y_1)$. Now (A9) shows that for a solution well behaved for large x , $\alpha(y) < \alpha(y_1)$ for $y < y_1$. Thus, we have immediately that

¹ There are many other ways to write this relation.

$$\alpha(y) > \alpha(y_1), \quad y > y_1, \quad (40)$$

so that *the friction in the outflow region must be larger than in the inflow region*. Accordingly, it is easier to choose $\alpha(y)$ for $y < y_1$ and use (39) to set $\alpha(y)$ for $y > y_1$.

4. A numerical example

As an example, we shall assume that $\alpha(y)$ is chosen arbitrarily for $y < y_1$ and use (39) to predict α when $y > y_1$. We consider three different specifications for $\alpha(y)$, $y < y_1$:

- (i) $\alpha(y) \equiv \alpha(y_1), \quad y < y_1$;
- (ii) $\alpha(y) = \alpha(y_1) \left(\frac{y - y_0}{y - y_1} \right), \quad y < y_1$;
- (iii) $\alpha(y) = \alpha(y_1) \left(\frac{y - y_0}{y - y_1} \right)^2, \quad y < y_1$.

(The last of these is taken as a rough approximation to the case of zero friction in the inflow region.) In all cases, we take a simple quadratic form for $h_I(y)$:

$$h_I(y) = h_m + (h_{\min} - h_m) \left(\frac{y - y_1}{y_0 - y_1} \right)^2, \quad (41)$$

where h_{\min} is the value taken at $y = y_0$. (This is not the minimum value of h_I , which occurs at the northern end of the gyre due to the asymmetry produced by ϵ .) We take $h_{\min} = 1$, $h_m = 1.2$, $\epsilon = 0.1$ (the form of the results does not depend qualitatively on the values chosen, as will be seen), and $y_0 = 0$, $y_1 = 1$. This choice gives $y_n = 2.07$.

Figure 2 shows the results for case (i). The dissipation coefficient α (Fig. 2a) varies between 0.083 for $y < y_1$ and 0.32 at the northern end of the gyre; progressively more friction is necessary the farther north one moves in the boundary layer. Figures 2b,c show h and v as functions of ψ at five different values of y . Note that for these parameters, v is everywhere quite small, although increasing $h_m - h_{\min}$ by a factor of 2 increases v by more than a factor of 4. Both h and v remain remarkably linear in ψ for all parameters tested. As functions of x (Figs. 2d,e) the situation changes; v in particular has an exponential-like behavior. In fact, the behavior of most quantities for large x is indeed exponential, as the Appendix shows.

This implies that had we chosen a D of the form κv (to be discussed in the next section), then κ would be approximately independent of x but would vary with y . In particular, a constant κ would not yield results matched to the specified interior. Figure 2f shows this clearly, by plotting the ratio D/v . Except near the center of the gyre, D/v is fairly uniform with x ; but its value varies with the north-south coordinate.

Figures 2g,h show the integrated dissipation E and the potential vorticity q . Note that q increases mono-

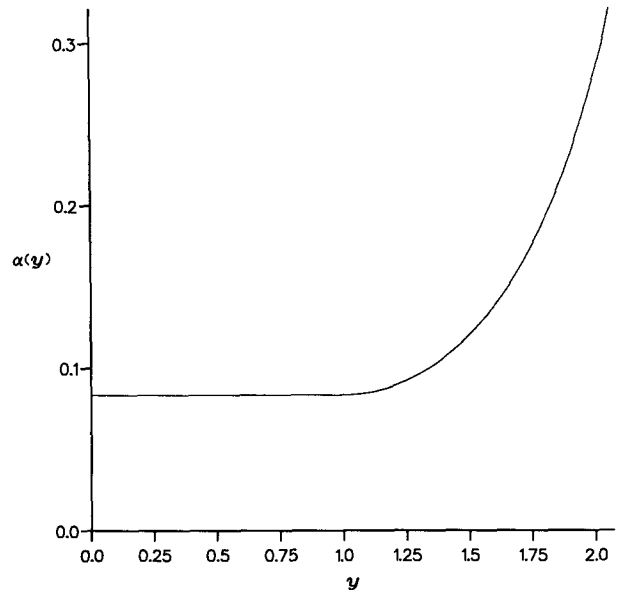


FIG. 2. Solutions for scheme (i). Shown are (a) the dissipation coefficient $\alpha(y)$, (b) h as a function of ψ for five values of y marked,

tonically with y everywhere, and along the western boundary it takes values that do not lie on any incoming streamline (it is for this reason that ψ , and not q , is a useful coordinate in the frictional case). The potential vorticity is approximately a linear function of ψ over most of the boundary layer for this case. Figure 2i then shows the circulation in the interior and boundary layer. The boundary layer appears to be narrower in the outflow region than farther south; but in both regions the nondimensional x extent is quite large.

Figure 3 shows some of the equivalent features for scheme (ii); those not shown are very similar to scheme (i). Decreasing α for $y < y_1$ by using this scheme produces an increase in α for y in the outflow region, but the changes are mostly small. There is an increase in the northward velocity v by up to 50% (Fig. 3a) and a narrowing of the boundary layer. The variation of D/v with x is now everywhere small; but its variation north-south is considerably stronger than in scheme (i); cf. Fig. 3b. The q field is now less linear, as Fig. 3c shows. Scheme (iii) gives very similar results to scheme (ii), and is not shown.

The detail of these results is less important than the conclusion, which can be drawn from them: *many different amounts of dissipation are capable of yielding boundary layer flows that match with a specified interior*, providing that the dissipation obeys a suitable equation.

The results apply qualitatively, even when parameters are varied. For example, the amplitude of the incoming u_I field was increased by setting $h_m = 1.5$; the differences are in the direction expected (e.g., the dissipation has increased, because the flow is more energetic). Another variation was to increase the beta

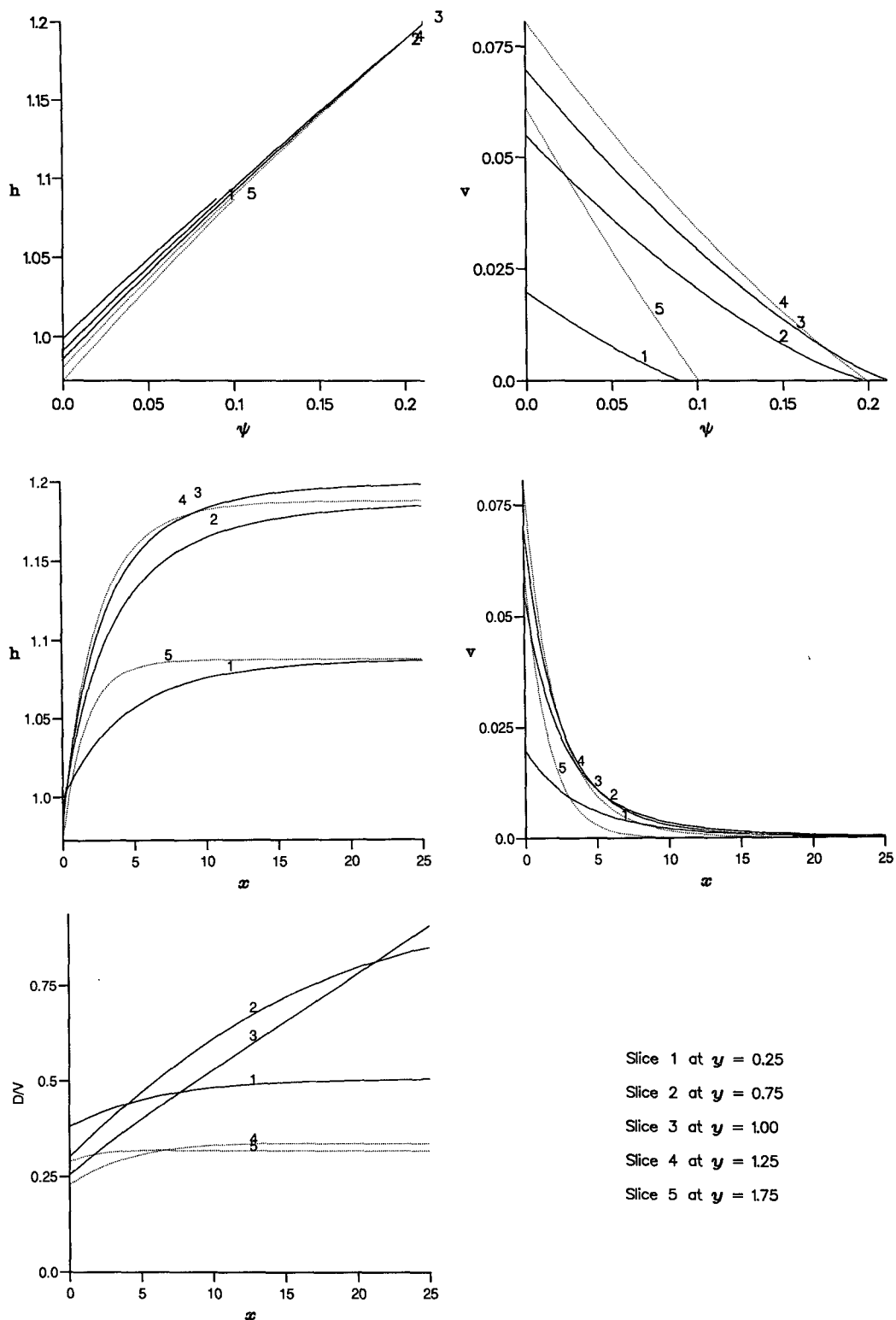


FIG. 2. (Continued) (c) v as a function of ψ for five values of y marked, (d) h , and (e) v as functions of x for the five values of y marked; (f) the ratio D/v as a function of x at the five values of y marked, (g) contours of the integrated dissipation E as a function of ψ and y , (h) contours of the potential vorticity q as a function of ψ and y , and (i) contours of the streamfunction ψ as a function of x and y .

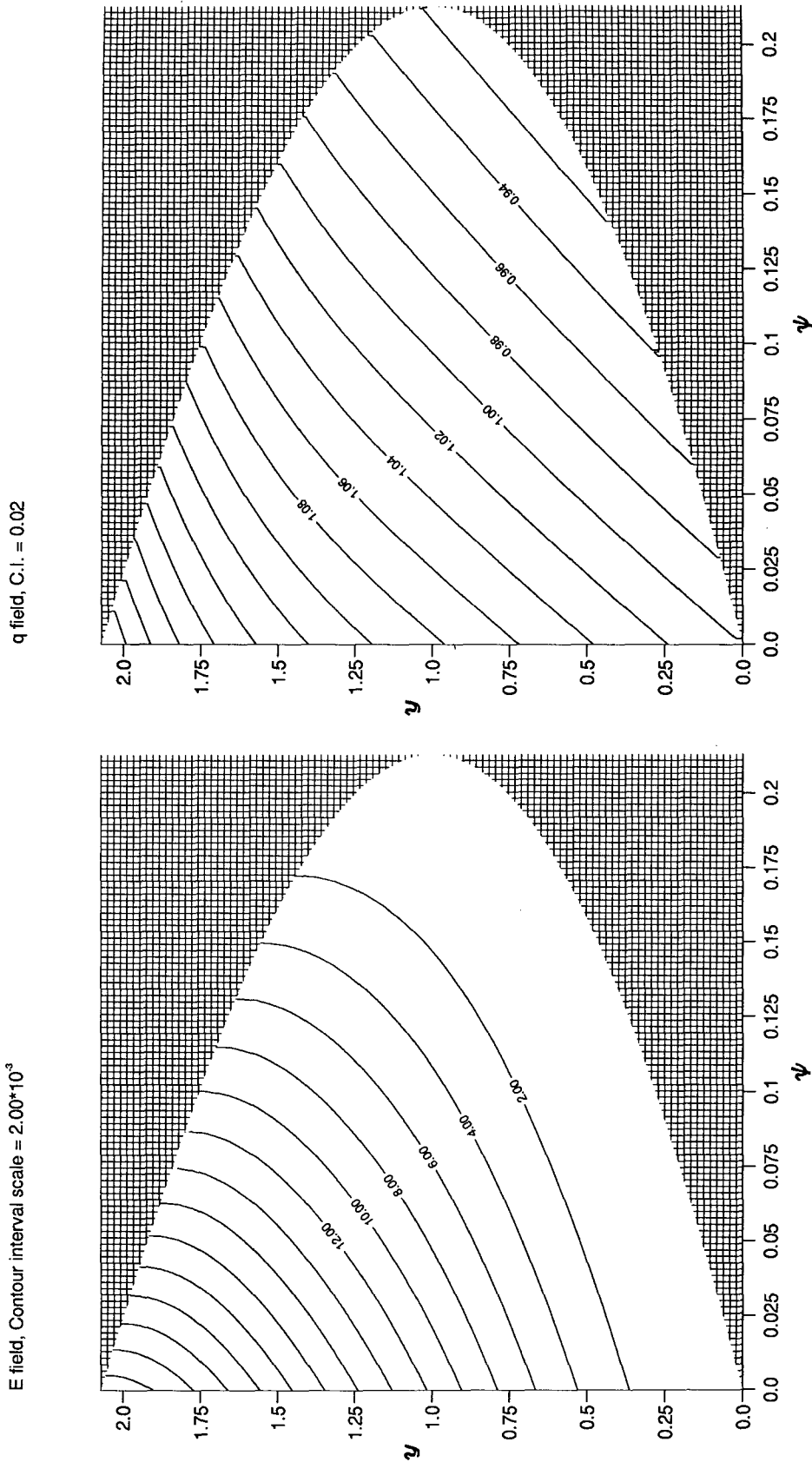


FIG. 2. (Continued)

ψ contours, C.I. = 0.010

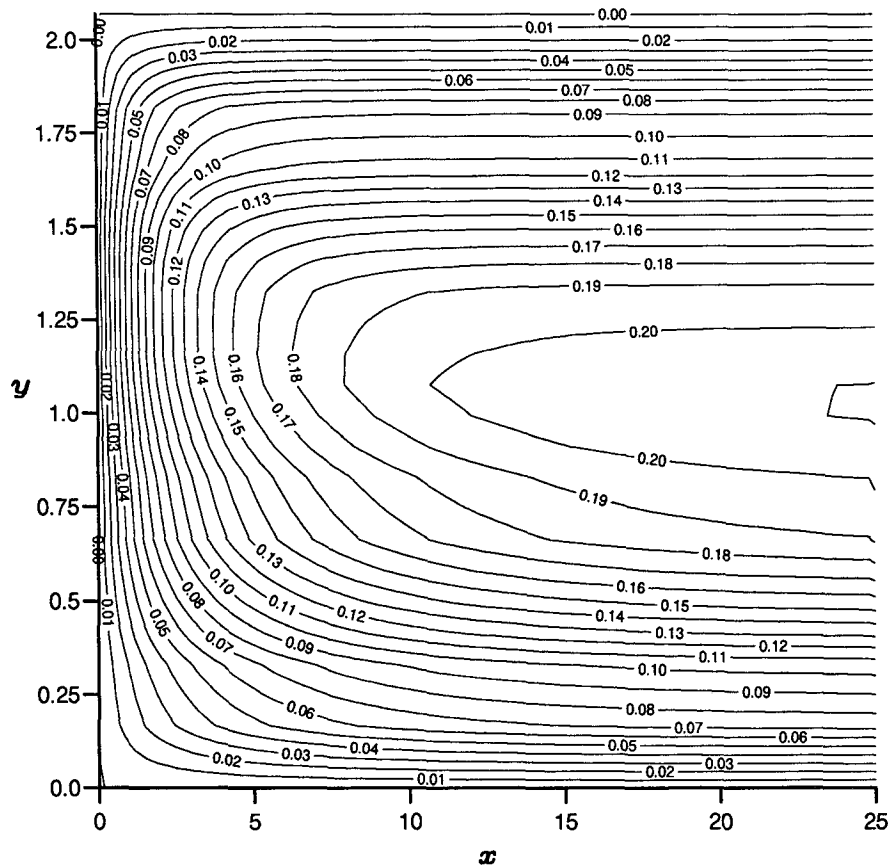


FIG. 2. (Continued)

term (i.e., ϵ) to 0.3, which had the interesting effect (cf. Fig. 4) of making the incoming potential vorticity be almost uniform; however, this had little effect on the solutions.

5. Solutions for a specified form of dissipation

We have seen that various distributions of the amount of dissipation produce a boundary layer that can match a specified interior flow. However, whatever the dynamics acting in a real, or a model, western boundary layer the dissipation will be related in some fashion to the flow in the boundary current. So now we ask whether, for a specific form and amount of dissipation, the solution can still match a specified interior in the outflow region. (If the answer to this question is affirmative, we cannot, of course, necessarily deduce that the interior circulation must be independent of boundary layer details; for example, there are changes to the interior circulation in quasigeostrophic theory as friction parameters are modified; cf. Harrison and Stalos 1982.)

We maintain the problem at its simplest, by choosing a linear drag for the dissipation, that is,

$$D = -\kappa v, \tag{42}$$

where κ is now a specified constant (the case of a distributed drag $-\kappa v/h$ is similar). To solve the problem, we first consider the inflow region $y \leq y_1$. Now h is known as before, by (20), and v satisfies (25), which can be rewritten as

$$v v_y + \kappa v = \epsilon \frac{\psi_I - \psi}{h}, \tag{43}$$

which is an o.d.e. for v , since h and ψ_I are known as functions of y in this region. An initial condition is needed for (43). This is clearly that $v = 0$ when $\psi = \psi_I$; that is, $v = 0$ when $y = \hat{y}(\psi)$. This does not directly permit an integration since (43) is formally singular there, but the well-behaved solution is found by differentiating (43) w.r.t. y , so that

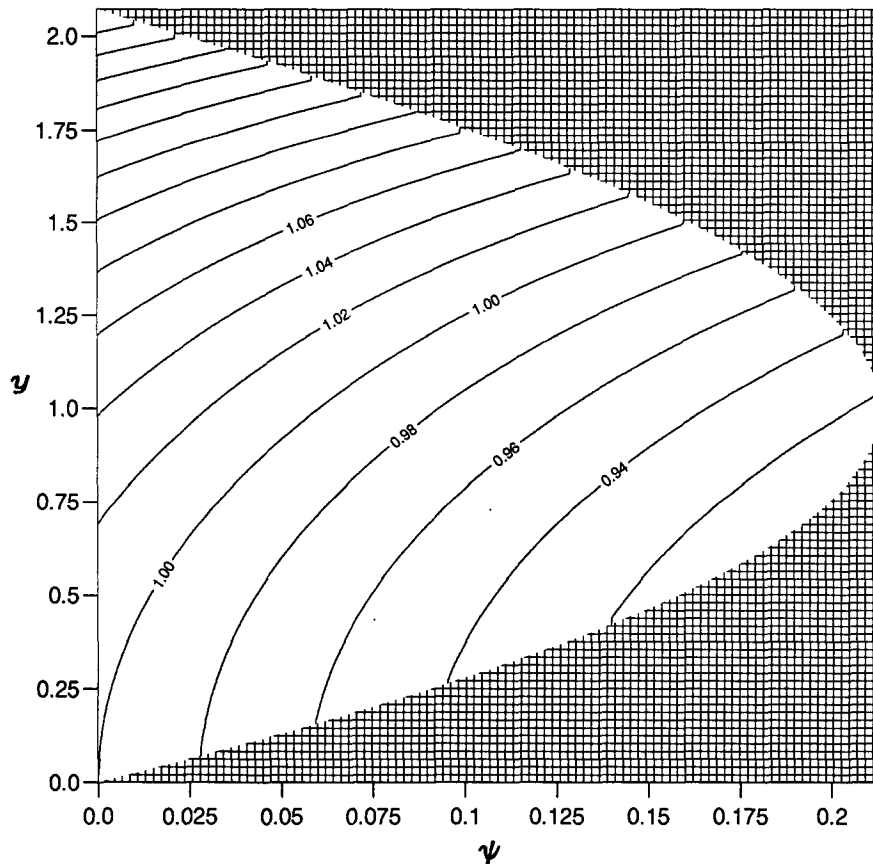
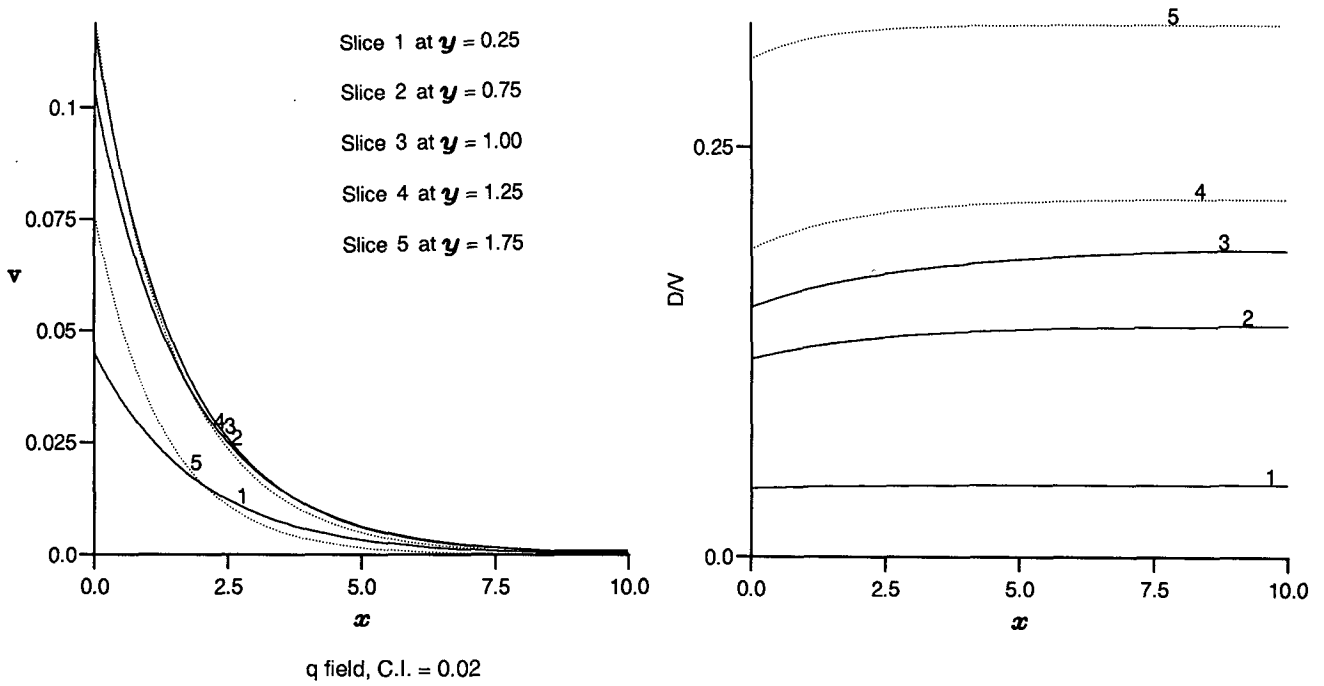


FIG. 3. Solutions for scheme (ii). Shown are (a) v as a function of x for the five values of y marked, (b) the ratio D/v as a function of x at the five values of y marked, and (c) contours of the potential vorticity q as a function of ψ and y .

q field, C.I. = 0.05

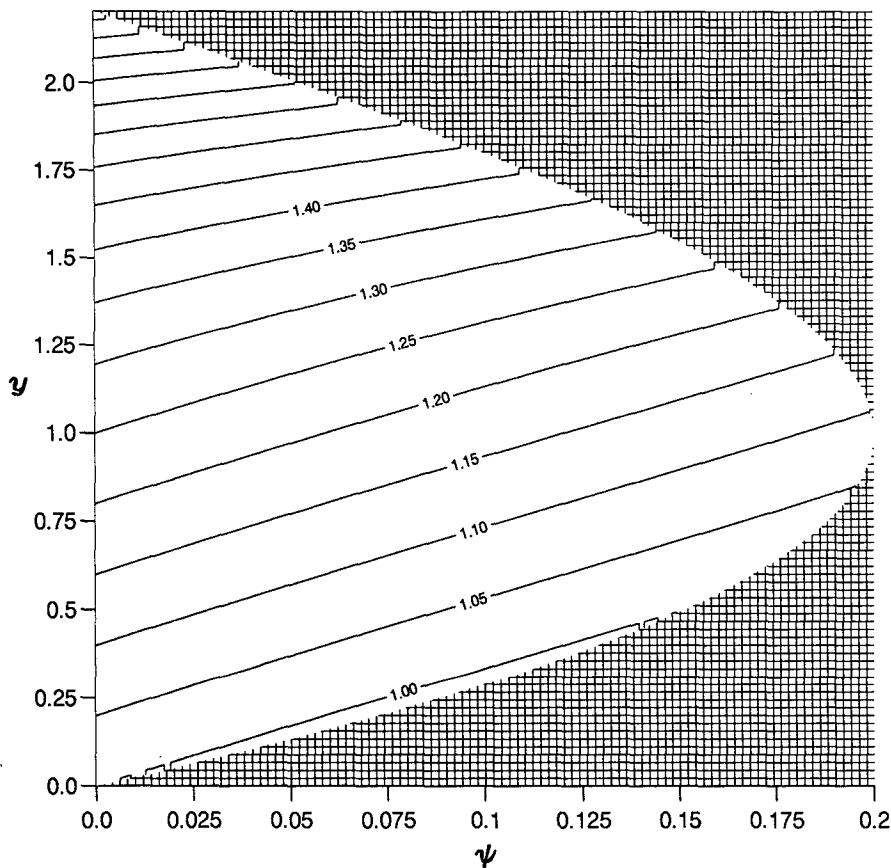


FIG. 4. Contours of the potential vorticity q as a function of ψ and y , for the case $\epsilon = 0.3$ (a stronger beta effect).

$$v_y = \frac{1}{2} \left[-\kappa \pm \left(\kappa^2 + \frac{4\epsilon h y}{f} \right)^{1/2} \right], \quad y = \hat{y}(\psi). \quad (44)$$

We can thus integrate v [and hence also find x , by (17)] northward until $y = y_1$.

If κ is sufficiently large that the v component of the flow is everywhere northward, then (43) may be integrated further, until v vanishes at a value of y where $\psi_I(y) = \psi$. The solution can then be constructed by integrating (17) to give x , as before.

However, this procedure is incomplete if κ is sufficiently small, because the N-S flow reverses in sign infinitely many times, qualitatively like the solutions of Cessi et al. (1990). The Von-Mises transformation is still valid, but its interpretation needs care. We adopt the approach of Page and Johnson (1991) and define a timelike variable τ , such that

$$v = \frac{dy}{d\tau}, \quad vv_y = \frac{d^2y}{d\tau^2}. \quad (45)$$

Equation (43) then becomes a second-order d.e. in τ for the northward position of a fluid parcel:

$$\frac{d^2y}{d\tau^2} + \kappa \frac{dy}{d\tau} = \frac{\epsilon(\psi_I - \psi)}{h} \equiv \epsilon h_y. \quad (46)$$

This can be integrated forward with pseudo-initial conditions $dy/d\tau = v(y_1)$, $y = y_1$ at $\tau = 0$. (Note that the integration cannot start at $y = \hat{y}$, since all terms and derivatives are zero there; the particle takes an infinite time to start and end its motion.)

Typical trajectories for large, medium, and small κ (0.5, 0.1, and 0.01) are shown in Figs. 5, 6, and 7. In the high-friction case (Fig. 5), the circulation pattern would closely resemble Fig. 2i [it would be arduous to compute enough (v, y) trajectories to derive the x field, and this has not been done here]. Each trajectory moves northward and becomes asymptotic to its interior value.

In the medium friction case (Fig. 6), the more energetic trajectories (those with smaller ψ ; i.e., those ini-

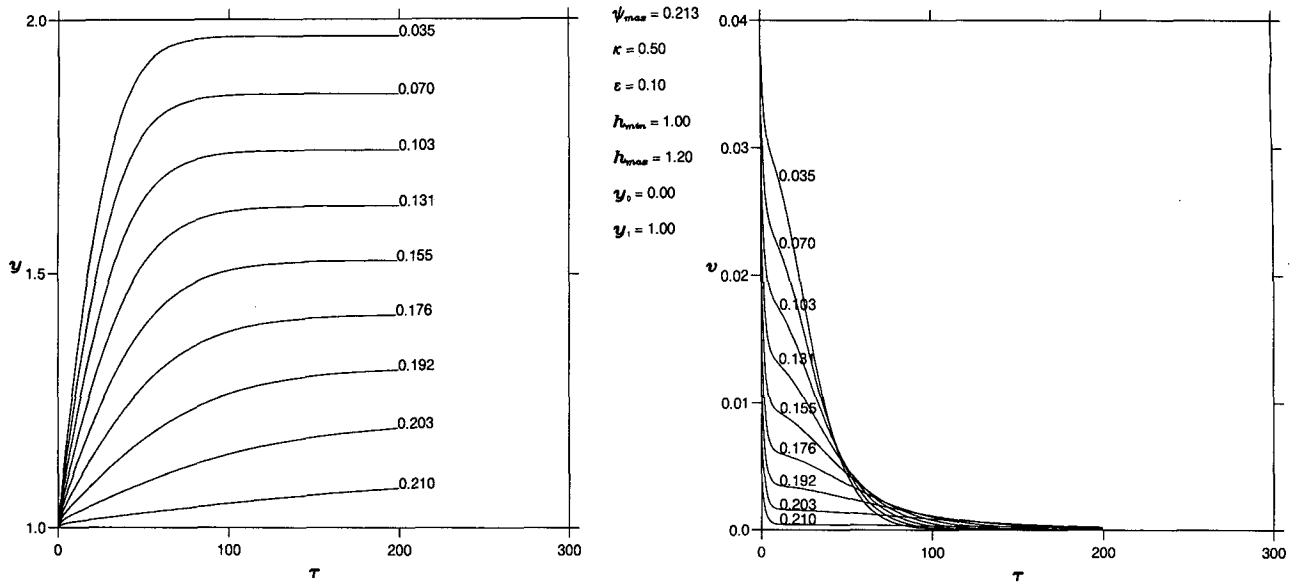


FIG. 5. Values of y and v (i.e., $dy/d\tau$) as functions of τ for a high friction case ($\kappa = 0.5$), showing a unidirectional boundary layer. Scheme (i) is used for the interior solution, with standard parameter values. Shown are (a) y and (b) v . The values of streamfunction ψ are indicated.

tially at the southern end of the gyre) overshoot their asymptotic positions and oscillate several times (with, therefore, both northward and southward velocities) before attaining their asymptotic position. These oscillations resemble damped standing planetary waves (cf. the Appendix). Finally, the low-friction case (Fig. 7) shows strong oscillations that are only weakly damped.

Provided that the oscillations are not large, the motion is damped simple harmonic motion, since the rhs

of (46) can be approximated, for y near the value y_a , where $\psi_I(y_a) = \psi$, as $\epsilon\psi'_I(y_a)(y - y_a)/h_I(y_a)$. The extent of the oscillations north-south can be estimated, when κ is small, by neglecting it to leading order. Then (43) integrates to (27), with E zero, so that v is $O(1)$ when y reaches its interior value. Accordingly, the north-south extent is also $O(1)$ (i.e., of order L dimensionally) independent of κ .

This is in direct contrast to the findings of Cessi et al. (1990), who found the northward overshoot

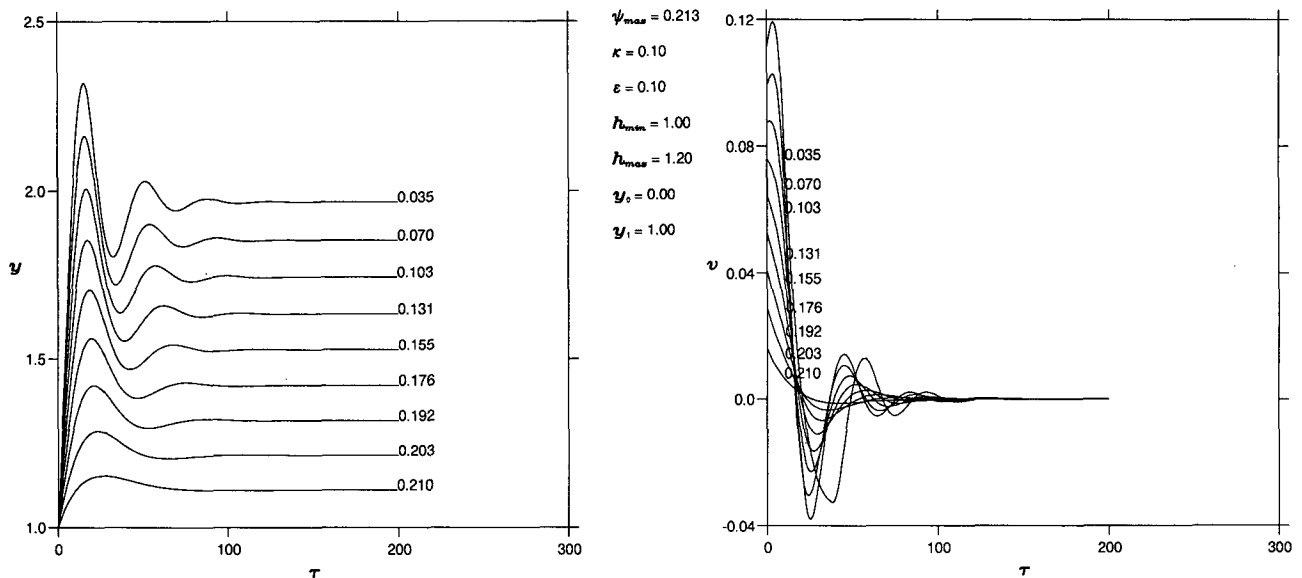


FIG. 6. As in Fig. 5 but for a medium friction case ($\kappa = 0.1$). Note the flow reversals.

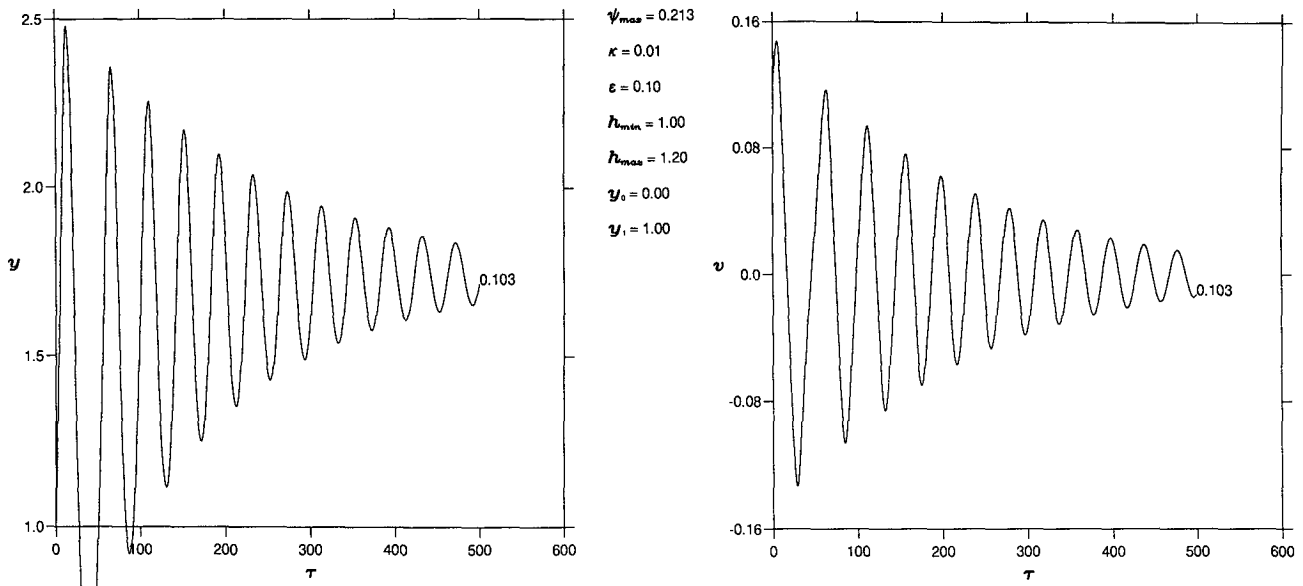


FIG. 7. As in Fig. 5 but for a low friction case ($\kappa = 0.01$). Only one value of streamfunction is shown, for clarity.

lengthened as $\nu^{-2/3}$ as lateral viscosity ν became small. Their interpretation was that the main dissipation occurred in the overshoot in their model, and not in the “loops” as the fluid approached the interior. In our linear drag case, the dissipation occurs instead in the (possibly unidirectional and possibly oscillatory) approach to the interior, and not in the overshoot. Thus the manner in which the low potential vorticity carried by the fluid adjusts to the interior occurs in the current model rather more as Pedlosky’s (1987) suggestion.

Despite the differences in the dynamics, however, both Cessi et al. (1990) and this study suggest that an inertial boundary layer can match to a specified interior flow for a given form (and value) of dissipation. However, neither our study, Cessi et al. (1991) or Page and Johnson (1991) prove this completely; a lengthy basinwide numerical study similar to that of Harrison and Stalos (1982) would be necessary to close the argument; such a study is beyond the scope of this paper.

An overestimate for the overshoot for any ψ can be found from (27). Equation (46) is well behaved as κ becomes small; it resembles nonlinear undamped simple harmonic motion. The approach to $\kappa = 0$ is linear, as can easily be shown (the same is true for the Page and Johnson analysis). For zero κ , v vanishes at a value of y when

$$h_I(\hat{y}) = h(y, \psi), \quad (47)$$

which will not be the interior in general. Now the (h, ψ) relationship (20) holds even for oscillatory flow, (when ψ may be greater than ψ_I), so we can scan y values until (47) is satisfied. For the streamline in Fig. 7, this yields $y = 2.54$, which is in excellent agreement.

In Figs. 6 and 7, the overshoot takes fluid particles beyond the northern boundary of the gyre and hence,

into the next gyre poleward, which is assumed to have the same analytic form as before (values of y that make h_I negative are not achieved by the solution). The interaction with this gyre will involve a patching of several boundary layers [see Page and Johnson (1991) for a simpler case] and is not considered here. At the very least, there will be modifications to many of the pathways found by this method.

In Fig. 7, also, the southward overshoot implies that there will be decaying oscillations in the *inflow* region. This problem is more awkward and has been avoided by the papers cited here. We have assumed that the approach to the boundary layer from the interior in the inflow region is a gradual monotonic change. If large-amplitude oscillations from the outflow region intrude into the inflow region, then the interior inflow solution is no longer known. The situation is unclear and will not be discussed here.

6. Conclusions

In this paper two related aspects of the role of friction in an inertial western boundary current are investigated. First, we have shown that many different amounts of dissipation can yield a unidirectional boundary current that can match a specified interior flow; all that is necessary is that the dissipation be suitably small in the inflow region and suitably large in the outflow region. Second, even if the dissipation has a specified form, solutions remain possible. When the size of the dissipative coefficient becomes small, inertial overshoot occurs and the flow becomes bidirectional, qualitatively similar to the solutions of Cessi et al. (1990). However, in their solution the overshoot lengthened as the friction decreased, so that the relevant

amount of dissipation had time to occur; in the solution here, there is a limit on the length of overshoot that is independent of dissipation. As a result, the dissipation must act in the damped oscillatory part of the solution as the interior is approached.

Using either approach, we have found, in agreement with Cessi et al. (1990), that the nonlinear boundary-layer solution, with the addition of eddy friction terms in various forms, is capable of matching to a specified interior solution. The evidence from this work, then, is that the simple western boundary layer structures considered here do not require that the ocean interior be related to the dynamics of the boundary layer itself. Put another way, it appears that the western boundary layer can be entirely passive as far as interior thermocline dynamics are concerned (it has *not* been proven that the western boundary layer *is* passive, however). The damped planetary wave can extend an appreciable distance into the interior; in both the Cessi et al. idealized calculation and this model, the length scale for the planetary wave distance is $(U/\beta)^{1/2}$ (cf. the Appendix).

These similarities and differences with Cessi et al. demonstrate that the polite fictions used to model the effects of turbulence in a western boundary current can have important effects on the dynamics; it is clear that more research into the parameterization of the turbulence is necessary.

The Von-Mises technique of using a streamfunction as an independent coordinate means that the problem of semigeostrophic flow with a prescribed inflow condition is essentially solved for the 1/2-layer problem, since the cross-stream coordinate may always be computed after the fact. However, the technique does not easily extend to two active layers, as Huang (1990) shows. Further, the treatment for a continuously stratified system remains notoriously difficult.

Acknowledgments. Bram Hauer provided the diagrams and numerical solutions in this paper. Ted Johnson suggested the line in section 5. A referee provided much useful debate and distinctly improved the paper.

APPENDIX

The Behavior near the Interior

a. The general case

Returning to a dimensional system, we may follow Moore (1963) and linearize Eq. (14) for q about the interior solution $v = 0$, $u = u_I(y)$, which yields to leading order

$$u_I v_{xx} + \beta v + D_x = 0, \quad x \rightarrow \infty. \quad (A1)$$

If the dissipation could be sufficiently small that it would play no role in this equation, then (A1) shows that when u_I is positive (i.e., when there is outflow from the boundary layer), there would only be an os-

cillatory solution for v , which does not decay. Thus, D must enter the balance in (A1) to leading order (an example of which is given in Cessi et al. 1990). In the case of inflow when u_I is negative, D can be zero, since there would still be a solution decaying eastward; hence the existence of friction is not *necessary* in the inflow region.

If D is given by

$$D = \kappa v \quad (A2)$$

for some linear drag κ , then v varies as $\exp(\alpha x)$, where α is a root of

$$u_I \alpha^2 + \kappa \alpha + \beta = 0,$$

whose roots are real (both negative) if $\kappa^2 > 4u_I\beta$, giving an exponential decay for v . If κ is smaller than this value, the solutions decay oscillatorily and v will have both positive and negative values, which case is considered in section 5. If we take as typical values $u_I \sim 1.5 \times 10^{-2} \text{ m s}^{-1}$, $\beta \sim 10^{-11} \text{ m}^{-1} \text{ s}^{-1}$, then κ must be larger than $8 \times 10^{-7} \text{ s}^{-1}$ for a nonoscillatory boundary layer. This value is fairly typical in the literature and corresponds to a Stommel width (κ/β) of 80 km.

However, if the drag is given by

$$D = -\nu v_{xx}, \quad (A3)$$

then the decay coefficient α satisfies the cubic

$$-\nu \alpha^3 + u_I \alpha^2 + \beta = 0,$$

which only possesses damped oscillatory solutions; this case is considered by Cessi et al. (1990).

b. The solutions for linear D

It is also necessary to examine the behavior of the (section 3) solutions with linear D as x becomes large; that is, as ψ approaches its interior value ψ_I . Let us define the small quantity

$$\phi = \psi - \psi_I(y) \leq 0.$$

Then, expanding (20) gives

$$h \sim h_I + \frac{f}{h_I} \phi - \frac{f^2}{2h_I^3} \phi^2 + \dots \quad (A4)$$

We also know v from (27). We can expand this also, to give

$$v^2 = 2 \left\{ B(\psi_I) + \phi B'(\psi_I) + \frac{\phi^2}{2} B''(\psi_I) + \dots - h_I \right. \\ \left. - \frac{f}{h_I} \phi + \frac{f^2}{2h_I^3} \phi^2 + \dots - E \right\}. \quad (A5)$$

Let us first consider the case $y \leq y_1$. In this case the $O(1)$ and $O(\phi)$ terms cancel identically, leaving merely

$$v^2 = \phi^2 \left(B''(\psi_I) + \frac{f^2}{h_I^3} \right) - 2E. \quad (A6)$$

Now E is defined by (29) and (34), and is straightforward to show that for small ϕ it takes the value

$$E \sim \frac{\alpha(y)}{2\psi'_I} \phi^2$$

so that

$$v^2 \sim \phi^2 \left(B''(\psi_I) + \frac{f^2}{h_I^3} - \frac{\alpha}{\psi'_I} \right), \quad (A7)$$

which, together with the identity

$$B''(\psi_I) + \frac{f^2}{h_I^3} = \frac{\epsilon}{h_I \psi'_I},$$

gives

$$v^2 \sim \frac{1}{\psi'_I} \left(\frac{\epsilon}{h_I} - \alpha \right) \phi^2, \quad (A8)$$

which immediately limits the size of α in the range $y \leq y_1$:

$$\alpha < \frac{\epsilon}{h_I} \equiv \alpha(y_1). \quad (A9)$$

Thus, the friction cannot be too large in the southern half of the western boundary current.

Then we can write

$$\psi_x = \frac{1}{x_\psi} = v h \sim h_I \left(\frac{\epsilon - \alpha h_I}{h_I \psi'_I} \right)^{1/2} (\psi_I - \psi). \quad (A10)$$

(The apparent singularity when y reaches y_1 can be shown not to occur, and in fact the behavior with ϕ is similar; the algebra is, however, tedious and is not shown.) Solving (A10) gives

$$\psi \sim \psi_I - \psi_0(y) \exp \left[-x h_I \left(\frac{\epsilon - \alpha h_I}{h_I \psi'_I} \right)^{1/2} \right] \quad (A11)$$

for large x , for some unknown $\psi_0(y)$. Thus, the behavior of both ψ and v is a simple exponential decay with x .

The case $y > y_1$ gives similar results, but rather more lengthily. As before, the $O(1)$ and $O(\phi)$ terms cancel identically, so that v^2 is again $O(\phi^2)$. After some algebra involved in the value of E , we find

$$v^2 \sim \phi^2 \left(B''(\psi_I) + \frac{f^2}{h_I^3} - \frac{\alpha(\hat{y})}{\psi'_I(\hat{y})} \right) = \phi^2 K, \quad \text{say.} \quad (A12)$$

Now this is identical to (A7) save that f and h_I are evaluated at $y > y_1$. Since $f(y) > f(\hat{y})$ and $h_I(y) < h_I(\hat{y})$ under most conditions, the bracket in (A12)

is larger than that in (A7). Hence if (A7) is satisfied, (A12) is usually well behaved. Note that neither (A9) nor (A12) limit $\alpha(y)$ for $y > y_1$ [but see Eq. (40)].

Then we find that

$$\psi \sim \psi_I - \psi_0(y) \exp(-x h_I K^{1/2}) \quad (A13)$$

for large x , which is the same behavior as when $y < y_1$. It is, then, simple to show that u varies as

$$u \sim u_I + x L \exp(-x h_I K^{1/2})$$

(adopting the latter notation), for some K, L . In the y -momentum equation, the leading terms (other than the interior balance) are those of order x times the exponential, and these are purely geostrophic; the dissipative term is only of order exponential, and so does not enter at this order. Of course, the term balance in the vorticity equation has all terms of the same order, showing again that the dissipation must be of the same order as the other terms here.

REFERENCES

Bryan, F. O., and W. R. Holland, 1989: A high resolution simulation of the wind- and thermohaline-driven circulation in the North Atlantic Ocean. *Parameterization of Small-Scale Processes. Proc. 'Aha Huliko'a 89*, P. Muller and D. Henderson, Ed., Hawaii, Hawaii Inst. Geophys. 362 pp.

Cessi, P., R. V. Condie, and W. R. Young, 1990: Dissipative dynamics of western boundary currents. *J. Mar. Res.*, **48**, 677-700.

Charney, J. G., 1955: The Gulf Stream as an inertial boundary layer. *Proc. Natl. Acad. Sci.*, **41**, 731-740.

Fofonoff, N. P., 1954: Steady flow in a frictionless homogeneous ocean. *J. Mar. Res.*, **13**, 254-262.

Foster, M. R., 1985: Delayed separation in eastward, rotating flow on a β -plane. *J. Fluid Mech.*, **155**, 59-75.

Harrison, D. E., and S. Stalos, 1982: On the wind-driven ocean circulation. *J. Mar. Res.*, **40**, 773-791.

Huang, R. X., 1986: Solutions of the ideal fluid thermocline with continuous stratification. *J. Phys. Oceanogr.*, **16**, 39-59.

—, 1990: Matching a ventilated thermocline model with inertial western boundary currents. *J. Phys. Oceanogr.*, **20**, 1599-1607.

Killworth, P. D., 1987: A continuously stratified nonlinear ventilated thermocline. *J. Phys. Oceanogr.*, **17**, 1925-1943.

—, 1992: Flow properties in rotating, stratified hydraulics. *J. Phys. Oceanogr.*, **22**, 997-1017.

Luyten, J., J. Pedlosky, and H. Stommel, 1983: The ventilated thermocline. *J. Phys. Oceanogr.*, **12**, 292-309.

Moore, D. W., 1963: Rossby waves in ocean circulation. *Deep-Sea Res.*, **10**, 735-747.

Morgan, G. W., 1956: On the wind driven ocean circulation. *Tellus*, **8**, 301-320.

Munk, W. H., 1950: On the wind-driven ocean circulation. *J. Meteor.*, **7**, 79-93.

Page, M. A., and E. R. Johnson, 1991: Nonlinear western boundary current flow near a corner. *Dyn. Atmos. Oceans*, **15**, 477-504.

Pedlosky, J., 1987: *Geophysical Fluid Dynamics*, 2d ed. Springer Verlag, 710 pp.

Stommel, H., 1948: The westward intensification of wind-driven ocean currents. *Trans. Amer. Geophys. Union*, **99**, 202-206.

Welander, P., 1971: Some exact solutions to the equations describing an ideal fluid thermocline. *J. Mar. Res.*, **29**, 60-68.